The e-ASTROGAM mission: a major step forward for gamma-ray polarimetry

V. Tatischeff[a,*], A. De Angelis[b,c], C. Gouiffès[d], L. Hanlon[e], P. Laurent[f], G. M. Madejski[g], M. Tavani[h,i,j], A. Ulyanov[e], on behalf of the e-ASTROGAM Collaboration[k]

[a]Centre de Sciences Nucléaires et de Sciences de la Matière, IN2P3-CNRS/Univ. Paris-Sud, Université Paris-Saclay, F-91405 Orsay Campus, France
[b]Università di Padova and INFN, via Marzolo 8, I-35131 Padova, Italy
[c]LIP/IST, Av. Elias Garcia 14, 1000 Lisboa, Portugal
[d]Laboratoire AIM, UMR 7158, CEA/DRF, CNRS, Université Paris Diderot, IRFU/SAp, F-91191 Gif-sur-Yvette, France
[e]School of Physics, University College Dublin, Belfield, Dublin 4, Ireland
[f]Laboratoire APC, UMR 7164, CEA/DRF CNRS, Université Paris Diderot, Paris, France
[g]Kavli Institute for Particle Astrophysics and Cosmology, Department of Physics and SLAC National Accelerator Laboratory, Stanford University, Stanford, CA 94305, USA
[h]INAF-IAPS, Via del Fosso del Cavaliere 100, I-00133 Roma, Italy
[i]INFN Roma Tor Vergata, Via della Ricerca Scientifica 1, I-00133 Roma, Italy
[j]Dipertimento di Fisica, Universit di Roma "Tor Vergata", Via Orazio Raimondo 18, I-00173 Roma, Italy
[k]See http://eastrogam.iaps.inaf.it/

Abstract. e-ASTROGAM is a gamma-ray space mission proposed for the fifth Medium-size mission (M5) of the European Space Agency. It is dedicated to the study of the non-thermal Universe in the photon energy range from ∼0.15 MeV to 3 GeV with unprecedented sensitivity, angular and energy resolution, together with a groundbreaking capability for gamma-ray polarimetric measurements. We discuss here the main polarization results expected from e-ASTROGAM observations of active galactic nuclei, gamma-ray bursts, microquasars, and the Crab pulsar and nebula. The anticipated performance of the proposed observatory for polarimetry is illustrated by simulations of the polarization signals expected from various sources. We show that polarimetric analyses with e-ASTROGAM should provide definitive insight into the geometry, magnetization and content of the high-energy plasmas found in the emitting sources, as well as on the processes of radiation of these plasmas.

Keywords: gamma-ray astronomy, polarization, space mission, Compton telescope, pair creation telescope.

* Vincent.Tatischeff@csnsm.in2p3.fr

1 Introduction

Gamma-ray polarimetry can be a powerful diagnostic of the high-energy physics at work in cosmic sources emitting collimated outflows and jets (e.g. blazars, gamma-ray bursts, X-ray binaries) or with strong magnetic field (e.g. pulsars, magnetars). In addition, measuring the linear polarization of distant (i.e. cosmological) gamma-ray sources (blazars, gamma-ray bursts) is a means of studying fundamental questions of physics related to Lorentz invariance violation (Ref. 1). However, very few polarization results have been obtained in high-energy astronomy so far, due to the

This material is based upon work supported by the U.S. Department of Energy, Office of Science, under Contract No. DE-AC02-76SF00515.

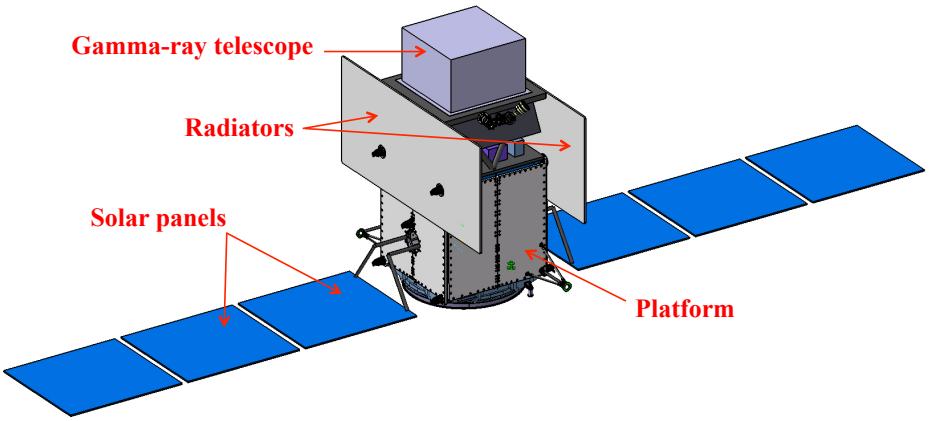

Fig 1 e-ASTROGAM spacecraft with solar panels deployed.

limited sensitivity of existing instruments to this observable.

The e-ASTROGAM mission concept aims to fill the gap in our knowledge of astronomy in the medium-energy (0.3-100 MeV) gamma-ray domain by increasing the number of known sources in this field by more than an order of magnitude and providing polarization information for many of them. Between 3000 and 4000 sources are expected to be detected during the first three years of mission operation. The e-ASTROGAM gamma-ray instrument inherits from its predecessors such as *AGILE*[2] and *Fermi*,[3] as well as from the MEGA prototype,[4] but takes full advantage of recent progress in silicon detectors and readout microelectronics to achieve excellent spectral and spatial resolution by measuring the energy and 3D position of each interaction within the detectors. The e-ASTROGAM mission concept is presented at length in Ref. 5. Here, we first give an overview of the proposed observatory (Sect. 2) and then outline the breakthrough capability of the e-ASTROGAM telescope for gamma-ray polarimetric observations of some of the main targets of the mission: active galactic nuclei (AGN), gamma-ray bursts (GRBs), the Crab pulsar/nebula system, and microquasars (Sect. 3).

2 The e-ASTROGAM observatory

The payload of the e-ASTROGAM satellite (Figure 1) consists of a single gamma-ray telescope operating over more than four orders of magnitude in energy (from about 150 keV to 3 GeV) by the joint detection of photons in both the Compton (0.15 – 30 MeV) and pair ($>$ 10 MeV) energy ranges. It is attached to a mechanical structure at a distance of about 90 cm from the top of the spacecraft platform, the space between the payload and the platform being used to: (i) host a time-of-flight (ToF) unit designed to discriminate between particles coming out from the telescope and those entering the instrument from below; (ii) host several units of the payload (the back-end electronics modules, the data handling unit, and the power supply unit) and (iii) accommodate two fixed radiators of the thermal control system, each of 5.8 m^2 area (Figure 1). This design has the advantage of significantly reducing the instrument background due to prompt and delayed gamma-ray emissions from fast particle reactions with the platform materials.

The e-ASTROGAM telescope is made up of three detection systems (Figure 2): a silicon Tracker in which the cosmic gamma-rays undergo a Compton scattering or a pair conversion (see Figure 2a); a Calorimeter to absorb and measure the energy of the secondary particles and an anticoincidence (AC) system to veto the prompt-reaction background induced by charged particles. The telescope has a size of 120$\times$120$\times$78 cm^3 and a mass of 1.2 tons (including maturity margins plus an additional margin of 20% at system level).

The Si Tracker comprises 5600 double-sided strip detectors (DSSDs) arranged in 56 layers. It is divided in four units of 5$\times$5 DSSDs, the detectors being wire bonded strip to strip to form 2-D ladders. Each DSSD has a geometric area of 9.5$\times$9.5 cm^2, a thickness of 500 μm, and a strip pitch of 240 μm. The total detection area amounts to 9025 cm^2. Such a stacking of relatively thin

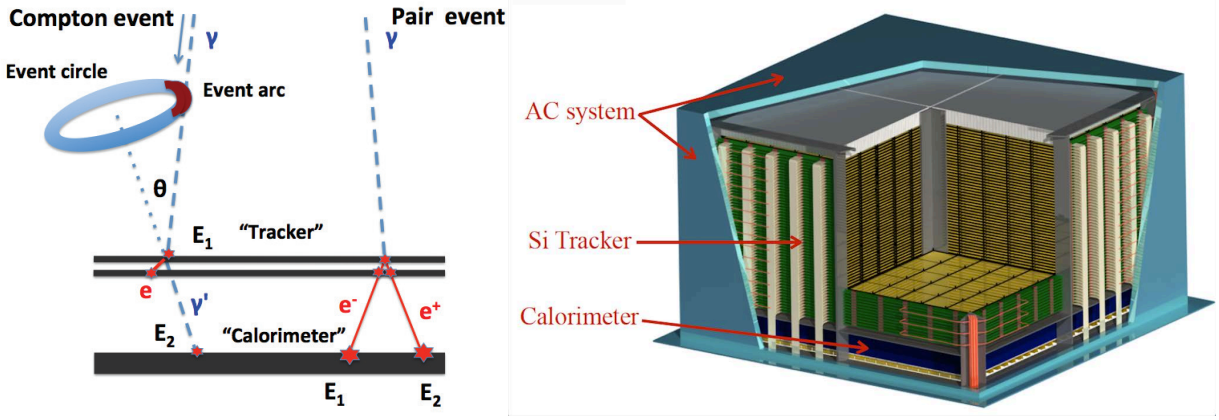

(a) (b)

Fig 2 (a) Representative topologies for a Compton event and for a pair event. Photon tracks are shown in pale blue, dashed, and electron and/or positron tracks are in red, solid. (b) Overview of the e-ASTROGAM payload.

detectors enables efficient tracking of the electrons and positrons produced by pair conversion, and of the recoil electrons produced by Compton scattering. The DSSD signals are read out by 860,160 independent, ultra low-noise and low-power electronics channels with self-triggering capability.

The Calorimeter is a pixelated detector made of a high-Z scintillation material – Thallium activated Cesium Iodide – for efficient absorption of Compton scattered gamma-rays and electron-positron pairs. It consists of an array of 33,856 parallelepiped bars of CsI(Tl) of 8 cm length and 5×5 mm^2 cross section, read out by silicon drift detectors (SDDs) at both ends, arranged in an array of 529 ($= 23 \times 23$) elementary modules each containing 64 crystals. The depth of interaction in each crystal is measured from the difference of recorded scintillation signals at both ends. Accurately measuring the 3D position and deposited energy of each interaction is essential for a proper reconstruction of the Compton events. The Calorimeter thickness – 8 cm of CsI(Tl) – makes it a 4.3 radiation-length detector having an absorption probability of a 1-MeV photon on-axis of 88%.

The third main detector of the e-ASTROGAM payload consists of an Anticoincidence sys-

tem composed of two main parts: (1) a standard Anticoincidence, named Upper-AC, made of segmented panels of plastic scintillators covering the top and four lateral sides of the instrument, requiring a total active area of about 5.2 m^2, and (2) a Time of Flight (ToF) system, aimed at rejecting the particle background produced by the platform. The Upper-AC detector is segmented in 33 plastic tiles (6 tiles per lateral side and 9 tiles for the top) coupled to silicon photomultipliers (SiPM) by optical fibers. The bottom side of the instrument is protected by the ToF unit, which is composed of two plastic scintillator layers separated by 50 cm, read out by SiPMs connected to Time Digital Converters. The required timing resolution is 300 ps.

For best environmental conditions, the e-ASTROGAM satellite should be launched into a quasi-equatorial (inclination $i < 2.5°$) low-Earth orbit (LEO) at a typical altitude of 550 – 600 km. The background environment in such an orbit is now well-known thanks to the Beppo-SAX[6] and *AGILE*[2] missions. In addition, such a LEO is practically unaffected by precipitating particles originating from solar flares, a virtue for background rejection.

Extensive simulations of the instrument performance using state-of-art numerical tools[7,8] and a detailed numerical mass model of the satellite together with a thorough model for the background environment have shown that e-ASTROGAM will achieve:[9]

- Broad energy coverage ($\sim$0.15 MeV to 3 GeV), with nearly two orders of magnitude improvement of the continuum sensitivity in the range 0.3 – 100 MeV compared to previous missions;

- Excellent sensitivity for the detection of key gamma-ray lines e.g. sensitivity for the 847 keV line from thermonuclear supernovae 70 times better than that of the *INTEGRAL* spectrometer (SPI);

- Unprecedented angular resolution both in the MeV domain and above a few hundreds of MeV i.e. improving the angular resolution of the COMPTEL telescope on board the *Compton Gamma Ray Observatory* (*CGRO*) and that of the *Fermi*/LAT instrument by a factor of $\sim$4 at 5 MeV and 1 GeV, respectively (e.g. the e-ASTROGAM Point Spread Function (68% containment radius) at 1 GeV is 9').

- Large field of view ($>$ 2.5 sr), ideal to detect transient Galactic and extragalactic sources, such as X-ray binaries and gamma-ray bursts;

- Pioneering polarimetric capability for both steady and transient sources, as illustrated in the next Section.

3 Polarimetry with e-ASTROGAM

e-ASTROGAM will be sensitive to the linear polarization of incident gamma-rays over its entire bandwidth. In the Compton range, the polarization signature is reflected in the probability distribution of the azimuthal scatter angle. In the pair production domain, the polarization information is given by the distribution of azimuthal orientation of the electron-positron plane. e-ASTROGAM will have a breakthrough capacity for gamma-ray polarimetry thanks to the fine 3D position resolution of both the Si Tracker and the Calorimeter, as well as the light mechanical structure of the Tracker, which is devoid of any heavy absorber in the detection volume.

The measurement of polarization in the pair creation range, using the azimuthal orientation of the electron-positron plane, is complex and a precise evaluation of the unfolding procedures and performance requires accurate simulation and testing.[10] In the following, we focus on the e-ASTROGAM performance for polarimetry in the Compton domain. We discuss in particular the

polarimetric capability of e-ASTROGAM for the study of active galactic nuclei (AGN), gamma-ray bursts (GRBs), the Crab pulsar and nebula, as well as microquasars.

3.1 Active galactic nuclei

Many, if not all, galaxies contain a massive central black hole, with masses ranging from a million to several billion times that of the Sun, but not all galaxies containing black holes are currently active. Specifically, we call a galactic nucleus "active" if it contains a bright and compact source of optical radiation (and is often, but not always, detected in other radiation bands). AGN revealing jet-like outflows in the optical band (about 10% of all AGN) are always strong emitters in the radio band. Blazars are sources where the jet points at (or close to) our line of sight, and the jet radiation being Doppler-boosted can dominate the emission from the accretion disk. Sources possessing a jet which points away from our line of sight often show gamma-ray emission, but at a level significantly weaker than blazars. For sources devoid of jets, the nuclear emission is dominated by thermal or quasi-thermal radiation from the black-hole accretion disk. The lack of a jet manifests itself by weak or absent emission in the radio and in gamma-rays, and these are Seyfert galaxies, or ordinary "radio-quiet" quasars. For a recent overview of taxonomy of gamma-ray emitting AGN, see Ref. 11.

The origin and the level of polarization in the hard X-ray/soft gamma-ray band for the radio-quiet sources (presumably associated with the accretion disk) and blazars (presumably associated with the jet) are quite different and are discussed separately.

3.1.1 Radio-quiet quasars and Seyfert galaxies

While these sources are copious emitters of soft to mid-range X-rays, they are not strong emitters of gamma-rays in the multi-MeV to GeV range.[12] The only radio quiet AGN detected by *Fermi*/LAT are Seyfert galaxies that happen to be also characterized by strong starburst activity, which in turn correlates with the star-formation rate,[13] so the accretion disk is not a likely source of GeV gamma-rays. On the other hand, Seyfert galaxies are often strong emitters of soft gamma-rays, and a number of them were detected by the *GCRO*/OSSE experiment[14] and subsequently by *INTEGRAL*.[15] Their spectra extend to several hundred keV, and as such, they are likely to be detected at the lower energy range of e-ASTROGAM: good bright examples are the Seyfert 1 galaxies NGC 4151 and IC 4329a, and the Seyfert 2 galaxy NGC 4945, all of them detected at ~ 200 keV (but with steep spectra, falling with energy). In all cases, the X-ray and soft gamma-ray emission is often seen to be variable (on time scales of roughly days, depending on the source), and such variability constrains the size of the X-ray emission region.

Our current best model for the formation of the X-ray spectra in these sources is Compton upscattering of the soft (UV-range) accretion disk photons – generated via quasi-thermal dissipation in the disk – to X-ray energies by a trans-relativistic plasma located as a corona above the accretion disk, or possibly some axially-symmetric proto-jet. The details of the geometry of the Compton-scattering medium are not known, but one would expect that any such sources – when viewed away from the axis of symmetry – would show polarization (because of the angular distribution of Compton scattering), and the angle of polarization would provide additional, important hints regarding the geometry of the Comptonizing medium. This is in addition to the crucial information about the temperature of the Comptonizing plasma, which can be gleaned from shape of

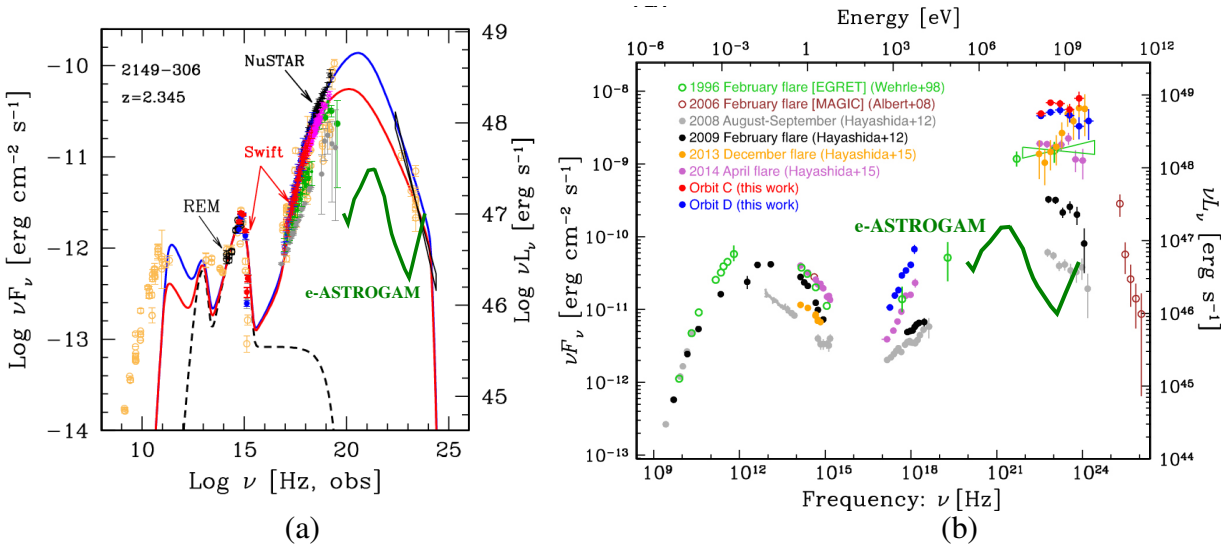

Fig 3 Spectral energy distributions of two FSRQ blazars together with the e-ASTROGAM sensitivity. (a) PKS 2149-306, which is at a redshift of 2.345, and the model of Ref. 16. (b) A collection of different spectral states of 3C 279 showing the dramatic gamma-ray flaring activity of this blazar.[17] The e-ASTROGAM sensitivity is for a source exposure of 1 yr in panel (a) and 1 day in panel (b).

the emission spectrum in the X-ray to gamma-ray range.

3.1.2 Jet-dominated active galaxies (blazars)

Broad-band emission from blazars is quite different to that from radio-quiet, accretion-dominated sources. Here, the emission extends to much higher energies: blazars are generally detected throughout the *Fermi* band (with clear detections in the 0.05 - 50 GeV range). The radio emission is extremely compact (with structures as small as milli-arcsecond, corresponding to sub-parsec scales), and is strongly polarized. The optical emission is highly variable, and often also strongly polarized. The optical spectra often (but not always) show emission lines, most clearly discernible when the sources are optically faint. Without exception, blazars are sources of X-ray emission. Measurement of polarization in the X-ray to gamma-ray range provides crucial insight not only to the geometry of the emitting region, but also allows to discriminate among various processes proposed as emission mechanisms.

For most blazars, their spectra, when plotted in the νF_ν representation, show two prominent broad humps, one peaking (depending on the source) at mm-to-soft X-ray band, and the other peaking in the gamma-ray band (Figure 3). We note that the mid-range gamma-ray emission is poorly studied, owing to the limited sensitivity of instruments flown so far. High levels of polarization measured for the low-energy hump, often exceeding 20% – together with frequently observed rapid polarization variability – argues for the emission process to be via the synchrotron mechanism. The high-energy peak is thought to originate via the inverse Compton process, presumably by the same electrons that produced the synchrotron hump. All this takes place in a volume that can be estimated from variability time scales. Broad-band spectra of blazars are successfully modeled by such synchrotron + inverse Compton models. However, while generically such a model appears to be applicable for all blazars, there are differences depending on the luminosity of the blazar.

In the luminous objects – often characterized by prominent optical and UV emission lines, and known as Flat Spectrum Radio Quasars, or FSRQs – the source of "seed" photons for Compton scattering is likely to be from the direct or reprocessed emission from the accretion disk, and most likely is provided by the optical/UV emission line-producing clouds (Ref. 18). In addition, the diffuse infrared radiation provided by the torus is also likely to be a significant source of "seed" photons.[19] Such radiation is not expected to be polarized. However, especially at the lower end of the high-energy peak (meaning in the X-ray band), the source of "seed" photons might be the synchrotron emission in the jet, as is the case for low luminosity objects.

In low-luminosity sources, the emission from the accretion disk and/or emission line clouds is weak (often undetectable). Those are the lineless BL Lac objects and the dominant source of the "seed" photons for inverse Compton scattering is most likely the synchrotron radiation produced in the jet.

A good overview of the polarization signature expected in the hard X-ray/soft gamma-ray bands is provided in Ref. 20. The level of polarization depends obviously on the emission process responsible for radiation in the band under consideration. For FSRQ-type blazars, the e-ASTROGAM 0.15 - 3000 MeV range corresponds, in all current scenarios, to the inverse Compton peak (see Figure 3a). If the "seed" photons are polarized, it is expected that the inverse Compton emission of photons upscattered via Comptonization should also show some level of polarization, but probably less than the synchrotron photons emitting in the optical/UV band. If those "seeds" are not polarized, there should be no discernible polarization in the up-scattered photons. Here, the measurement of polarization would be the "smoking gun" for the origin of the "seeds" for Comptonization. Polarization of hard X-rays/soft gamma-rays would implicate the synchrotron process internal to the jet. If no polarization is detected – this would support the radiation external to the jet. An intriguing possibility is that the rapidly variable component of gamma-ray emission during rapid and luminous outbursts of FSRQ blazars (such as 3C 279; see Figure 3b) might be synchrotron emission from the most energetic electrons (Refs. 17, 21). In that case, the polarization of gamma-ray emission during such outbursts should be very strong and readily measurable by e-ASTROGAM.

For BL Lac objects, hard X-rays are probably still dominated by the "tail" of the synchrotron process, so the polarization should be strong. Since there are very few measurements of BL Lac blazars in the spectral region where the e-ASTROGAM is sensitive, it is not clear where the "onset" of the high energy, inverse-Compton hump is located. If our current model for the broad-band spectra of BL Lacs is correct, one should see the broad-band spectra falling sharply (in νF_ν) up to several hundred keV, and rising again at even higher energies. We should see strong polarization associated with the falling spectrum (photon index > 2), weakening (but still discernible) at the

point where the spectrum breaks to photon index < 2. A more extensive and quantitative discussion is in papers by Chakraborty et al.[22] and Zhang et al.,[23,24] but qualitatively, the general picture outlined above is in agreement with those papers. In addition, Zhang et al.[23,24] have pointed out that gamma-ray polarization can provide definitive insight into the presence of hadrons in blazar jets, because hadronic models predict a much higher degree of polarization than leptonic models.

In summary, the sensitive spectroscopy and measurement of polarization in the e-ASTROGAM spectral range is crucial towards the understanding of emission models in all classes of AGN.

3.2 Gamma-ray bursts

Gamma-ray Bursts (GRBs) are the most luminous electromagnetic transients in the universe, with spectra that peak in the 0.1–1 MeV range. Their huge luminosities ($\sim 10^{51}$ erg in a narrow collimated jet) are emitted by the most relativistic jets known ($\Gamma > 100$) and are observed over a very short timescale (tens of seconds) at redshifts extending up to at least $z \sim 9$. The 'short' GRBs, with durations $\lesssim 2$ s are believed to originate from compact binary mergers (NS-NS, NS-BH), while those with durations $\gtrsim 2$ s ('long' GRBs) originate from the collapse of massive stars. GRBs are therefore powerful probes of the early universe, of fundamental physics, and of matter and radiation under the most extreme conditions.[25,26]

However, the nature of the central engines producing the relativistic jets in GRBs, the physical properties of the jets themselves, the energy dissipation sites and the radiation mechanisms, all remain poorly understood. In the black hole scenarios, the jet may be launched by the Blandford-Znajek mechanism, provided that sufficiently strong magnetic fields thread the black hole horizon. If the magnetic field does play an important role as an energy mediator in jet production, then a highly magnetized outflow close to the jet-launching site is expected and such a jet would be

magnetically dominated. In the case of synchrotron emission with ordered magnetic fields, the observed GRB polarization is expected to vary little with viewing angle. However, in the case of synchrotron emission in random magnetic fields and for Compton-drag models, the observed polarization should be significant only near the edge of the jet. These families of models can be distinguished by collecting a sufficiently large sample of GRBs with accurately measured polarization fractions.[27]

In GRBs the relativistic jets are optically thick in the launch region.[28] As the jets expand and become transparent, they release internally trapped photons as photospheric emission that has a distinctive polarization signature, which evolves during the GRB. Polarisation measurements as a function of energy and time can therefore discriminate between synchrotron and photospheric emission mechanisms in the prompt GRB phase.

SPI and IBIS on *INTEGRAL* have demonstrated the capability to detect the signature of polarized emission in the medium energy gamma-ray range from γ-ray sources, including GRBs. For example, GRB 041219a was an intense burst localized by *INTEGRAL*, whose degree of linear polarization in the brightest pulse of duration 66 s was found by SPI to be $63^{+31}_{-30}\%$ at an angle of 70^{+14}_{-11} degrees in the 100–350 keV energy range.[29] The same interval analysed using IBIS Compton mode data yields an upper limit on the polarisation fraction of $\leq 4\%$. The IBIS data for the intense first pulse of this exceptionally bright GRB was heavily affected by telemetry saturation, which may explain the disparity between the results from the two instruments. The polarisation results from SPI and IBIS for the brightest 12 s interval of the first pulse in this GRB are consistent with each other.[30] The relatively low significance of these detections ($\sim 3\sigma$), combined with the lack of on-ground calibration of polarimetric response to quantify systematic effects, limit the scope of what can be achieved with instruments that were not expressly designed for polarization

measurements.

The Gamma-Ray Burst Polarimeter (GAP) aboard the Small Solar Power Sail Demonstrator, IKAROS, launched in 2010, was the first instrument designed and calibrated for polarimetric GRB observations between 50–300 keV.[31] GAP notably detected GRB 100826A, with an average polarization degree of $27\% \pm 11\%$, $2.9\,\sigma$ confidence level.[32] The polarisation angle was observed to vary by $\sim 90^\circ$ during the prompt emission, which is difficult to explain for an axi-symmetric jet in the above scenarios. The polarisation swing during the burst can be interpreted as evidence for patchy emission, patchy magnetic field, or as photospheric emission from a variable jet. A further 2 GRBs were observed by GAP to have polarization degrees above 70%, but with no change in polarization angle,[33] consistent with magnetic field structures in the emission region being globally ordered fields advected from the central engine.

Several other soft γ–ray polarimetric instruments have been proposed, and are in various stages of implementation. For example, POET has been proposed to NASA as a SMEX mission with a science payload composed of two polarimetry instruments to make polarization and spectral measurements from about 2 keV up to about 500 keV.[34] POET's High Energy Polarimeter (HEP) instrument design derives from the balloon-borne polarimeter GRAPE (Gamma-RAy Polarimeter Experiment) that was successfully flown in 2011 and placed constraints on the polarization from the Crab Nebula and two M-class solar flares.[35] POLAR is a dedicated GRB polarimeter that has been proposed as a payload for the Chinese Space Laboratory. It is capable of detecting ~ 10 GRBs/yr with minimum detectable polarization (MDP) $\leq 10\%$.[36] The Astrosat mission, launched in September 2015, has a CZT imager[37] with the capability to make time resolved polarisation measurements for 5–6 GRBs per year.[38]

The left panel of Figure 4 shows the expected sensitivity of e-ASTROGAM for the detection

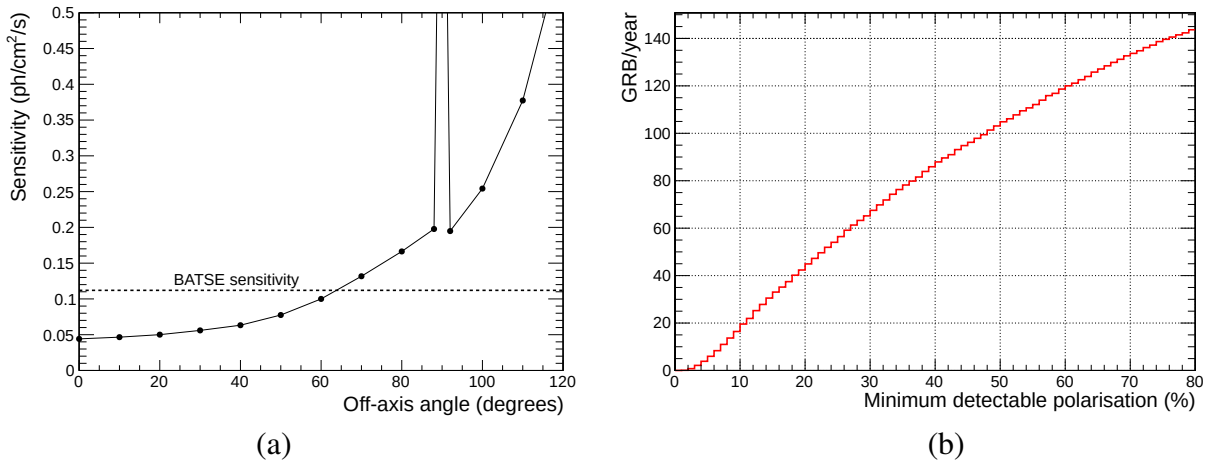

(a) (b)

Fig 4 (a) GRB flux sensitivity of e-ASTROGAM in the 0.2–2 MeV range on a timescale of 1 s. The dashed line shows the GRB flux corresponding to the 50% trigger efficiency of the BATSE instrument (0.29 photon cm^{-2} s^{-1} in the 50–300 keV range). (b) Cumulative number of GRBs to be detected by e-ASTROGAM as a function of the minimum detectable polarization MDP_{99} in the 150–300 keV range.

of GRBs in the 0.2–2 MeV energy range, as a function of the off-axis angle $\theta_{\mathrm{off-axis}}$. Here, the GRB emission spectrum has been approximated by a typical Band function[39] with $\alpha = -1.1$, $\beta = -2.3$, and $E_{\mathrm{peak}} = 0.3$ MeV. The e-ASTROGAM sensitivity is expected to be better than that of *CGRO*/BATSE for $\theta_{\mathrm{off-axis}} \lesssim 65^{\circ}$. Overall, the total number of GRBs detected by e-ASTROGAM is expected to be ∼600 in 3 years of nominal mission lifetime.

The strength of e-ASTROGAM regarding GRB polarimetry will be in its reliable polarization measurements for a large sample. The right panel of Figure 4 shows the number of GRBs detectable by e-ASTROGAM as a function of the minimum detectable polarization at the 99% confidence level (MDP_{99}) in the 150–300 keV band. The response of e-ASTROGAM to linearly polarized GRBs has been simulated at several off-axis angles in the range $[0^{\circ}; 90^{\circ}]$. For each value of $\theta_{\mathrm{off-axis}}$, the distribution of reconstructed azimuth scatter angles has been corrected for the asymmetry of the detector acceptance using a similar distribution obtained for an unpolarized source.

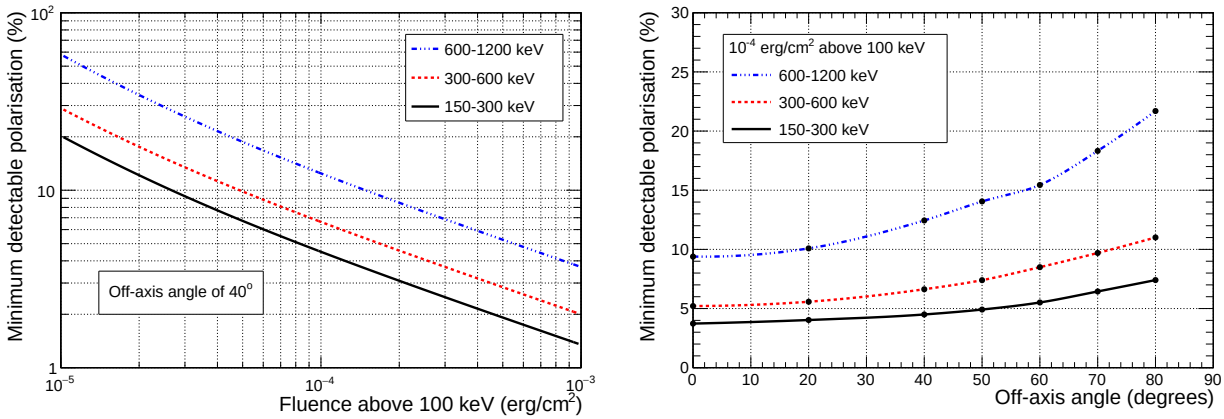

Fig 5 Minimum polarization fraction MDP_{99} detectable by e-ASTROGAM in three energy bands as a function of the GRB fluence (a) and as function of the off-axis angle (b). The GRB duration is assumed to be 50 s and the spectrum is a Band function with $\alpha = -1.1$, $\beta = -2.3$, and $E_{\mathrm{peak}} = 0.3\,\mathrm{MeV}$.

The minimum detectable polarization has been calculated as

$$\mathrm{MDP}_{99} = \frac{4.29}{\mu_{100} S}\sqrt{S+B}, \tag{1}$$

where μ_{100} is the modulation amplitude for a 100% polarized source, S and B are the number of source and background counts, respectively.[40] The number of GRBs with polarization measurable with e-ASTROGAM has then been estimated using the GRB fluences and durations from the Fourth BATSE GRB Catalog.[41] From Figure 4 it can be seen that e-ASTROGAM should detect a polarization fraction of 20% in about 40 GRBs per year, and a polarization fraction of 10% in $\sim$16 GRBs per year.

For bright GRBs (with fluence above 100 keV $\gtrsim 10^{-4}$ erg cm^{-2}), e-ASTROGAM will be able to measure polarization for several energy bands between 150 and 1200 keV (Figure 5). This polarization information, combined with spectroscopy over a wide energy band, will provide unambiguous answers regarding the origin of the GRBs' highly relativistic jets and the mechanisms

of energy dissipation and high-energy photon emission in these extreme astrophysical phenomena.

3.3 The Crab pulsar and nebula

The Crab nebula is the remnant of a star that exploded in 1054. The leftover neutron star, the Crab pulsar, has a rotation period of 33 milliseconds and spreads high-energy particles, up to 10^{15} eV, into the surrounding medium. Thanks to the energetic population of electrons in the pulsar wind, the compact nebula emits at all wavelengths, in particular at MeV energies by synchrotron radiation and at higher energies via inverse Compton scattering. The bright synchrotron radiation is particularly well suited for detailed studies of the inner region of the Crab pulsar/nebula system. For decades the flux from the whole nebula was expected to be constant and consequently this "standard candle" was observed by numerous space experiments for high-energy calibration purposes. This situation has changed in 2007 with the detection by the *AGILE* and *Fermi* missions of strong γ-ray flares.[42–44] Nevertheless, the precise localization of the emission inside the nebula and the physical origin of this sudden bright activity are not yet well understood, requiring more studies.

Polarized emission from the nebula and pulsar has been measured from radio to X-rays up to a few keV.[45] Recently, polarization in hard X-rays was detected with the two main instruments on board the *INTEGRAL* satellite, IBIS and SPI.[46,47] These polarimetric measurements give access to information related to the wind geometry and the magnetic field configuration in the pulsar environment, parameters that make it possible to constrain where and how efficiently particle acceleration takes place. In the MeV range, both the pulsar and nebular components of the system contribute significantly to the total emission. Thanks to the excellent sensitivity and timing resolution of the e-ASTROGAM telescope, phase-resolved polarimetric analysis will be possible,

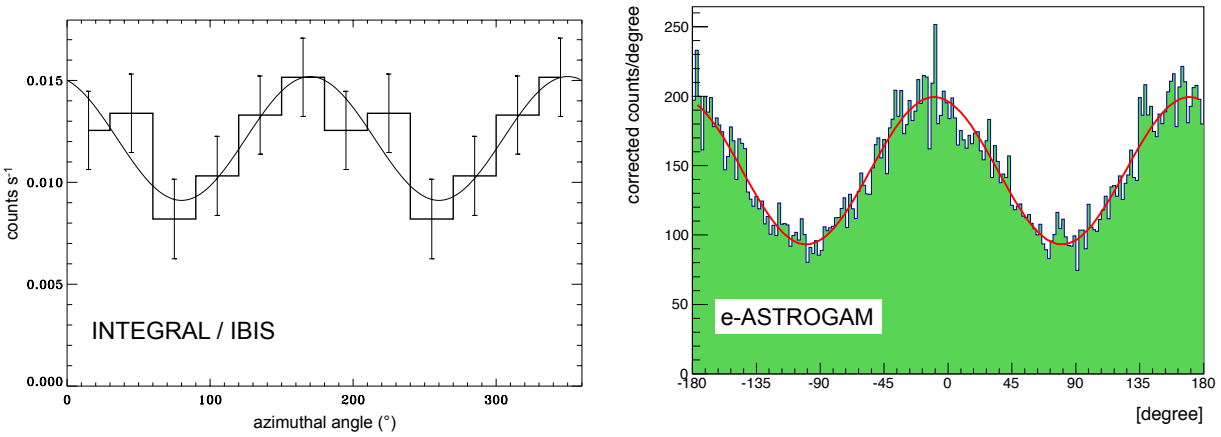

Fig 6 (a) Phase-averaged polarization diagram of the Crab pulsar and nebula obtained with *INTEGRAL*/IBIS in the 300 – 450 keV energy band by summing 1.831 Ms of data taken between 2012 and 2014 (adapted from Ref. 48). The measured polarization fraction and angle are PF $= (98\pm37)\%$ and PA $= 80°\pm12°$, respectively. (b) Simulation of the e-ASTROGAM polarization signal in the same energy band (300 – 450 keV) for an effective duration of observation of the Crab pulsar and nebula 100 times shorter than that accumulated by *INTEGRAL*/IBIS (i.e. $T_{\rm obs} = 1.831 \times 10^4$ s $\simeq 5$ h). The reconstructed polarization fraction and angle are PF $= (98.0 \pm 2.4)\%$ and PA $= 80.2° \pm 0.7°$.

allowing a detailed study of the compact inner nebula surrounding the Crab pulsar (the so-called pulsar wind nebula).

Figure 6 shows a comparison of a phase-averaged polarization diagram for the Crab pulsar and nebula obtained with *INTEGRAL*/IBIS[48] summing 1.831 Ms of data between 2012 and 2014 and a simulated polarigramme for e-ASTROGAM observation of the Crab region with 100 times shorter exposure ($T_{\rm obs} = 1.831 \times 10^4$ s). The improvement of the data quality with e-ASTROGAM is obvious (note the large increase in the number of bins made possible by the much higher statistics accumulated with e-ASTROGAM). For the simulations we used the Crab energy spectrum of Ref. 49 and assumed the central values measured with *INTEGRAL*/IBIS[48] for the polarization fraction (PF $= 98.0\%$) and angle (PA $= 80.0°$) of the soft gamma-ray emission ($\Delta E = 300$ – 450 keV). The simulated result shows that e-ASTROGAM will be able to provide a detailed gamma-ray view of the time-dependent polarization properties of the Crab nebula and pulsar, in particular during the

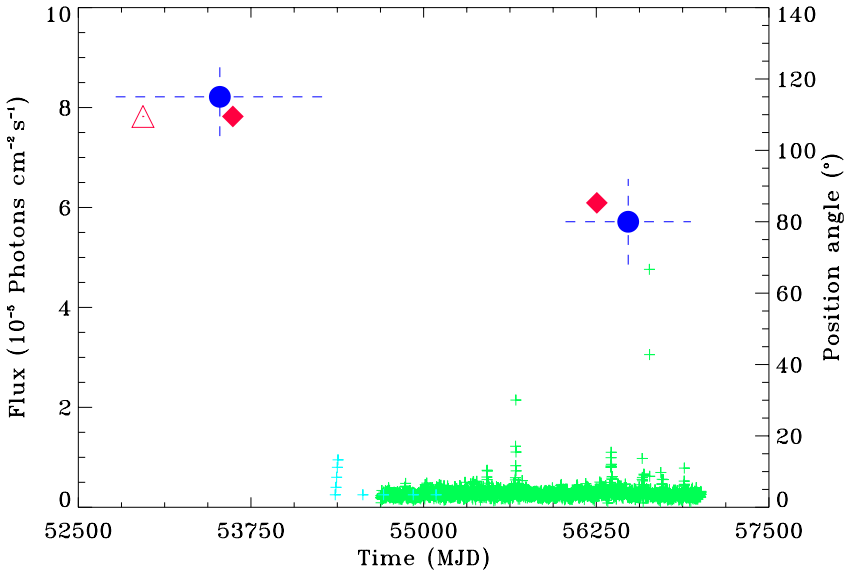

Fig 7 Crab light curve in the high-energy band (above 100 MeV) measured by *Fermi* and *AGILE* (green and cyan color) and polarization measurements obtained between 2003 and 2014 in the optical (red points) and in hard X-rays (300–450 keV) with *INTEGRAL*/IBIS (blue filled circles).[48] A similar change in the polarization position angle appears in both bands. e-ASTROGAM will determine the polarization properties of the system in the MeV range on a timescale similar to that of optical observations (∼hours).

periods of strong gamma-ray flaring activities possibly associated with magnetic reconnection.[42,43]

Combined polarimetric observations of the Crab pulsar/nebula system with *INTEGRAL* in hard X-rays and in the optical band with the Galway Astronomical Stokes Polarimeter (GASP) optical polarimeter have led to the suggestion that the polarization angle of both the visible and high energy light changed in a similar way over a year-long timescale.[48] This result was tentatively attributed to magnetic reconnection events as observed in the solar corona or detected in AGN[50] during bright high-energy flares. The e-ASTROGAM performance will definitively permit simultaneous MeV-optical observations, allowing a detailed study of these variations on a shorter timescale (Figure 7).

Polarimetric studies with e-ASTROGAM will help to better understand particle acceleration near compact objects, their injection and interaction in their close environment and the geometry and structure of the magnetic field in these systems. In coordination with highly-promising future

facilities in the optical and radio bands (E-ELT and SKA), the Crab pulsar/nebula system is the ideal target for such studies. Beyond this prime objective, the e-ASTROGAM mission will make it possible to study the polarimetric properties of pulsar wind nebulae and supernova remnant systems with different characteristics (e.g. energetics, age and magnetic field strength), including, for example, MSH 15-52 in our Galaxy and SNR 0540-69 in the Large Magellanic Cloud.

3.4 Microquasars

Black Hole Binaries (BHB) transit through different "spectral states" during their outbursts, the two canonical ones are the soft state (SS) and the "low" hard state (LHS). In the SS the emission is dominated by a bright and warm ($\sim$ 1 keV) accretion disk, the level of variability is weak, and the power density spectrum (PDS) is power-law like. No radio emission is detected in this state, and this is interpreted as an evidence for an absence of jets. In the LHS, on the other hand, the disk is much colder ($\sim$ 0.5 keV) and is thought to be truncated at a large distance from the accretor. The X-ray spectrum also shows a strong power-law like component extending up to hundred of keV, sometimes showing a roll-over at typically 50 – 200 keV. The level of rapid variability is much higher and the PDS shows a band-limited noise component, with sometimes quasi-periodic oscillations with frequencies in the range 0.1 – 10 Hz. During this state a "compact-jet" is detected mainly through its emission in the radio to infrared domain.

The BHB Cygnus X-1 (Cyg X-1) was discovered in 1964[51] and is the brightest binary in the sky, detectable in the MeV range. It is the first Galactic source known to host a black hole[52] (BH), and the most recent estimates led to a BH mass of 14.8 ± 1 solar masses. Cyg X-1 belongs to the family of microquasars owing to the detection of compact relativistic jets in the LHS,[53] and it is one of the (very few) microquasars known to have a hard tail extending to (and beyond) the MeV

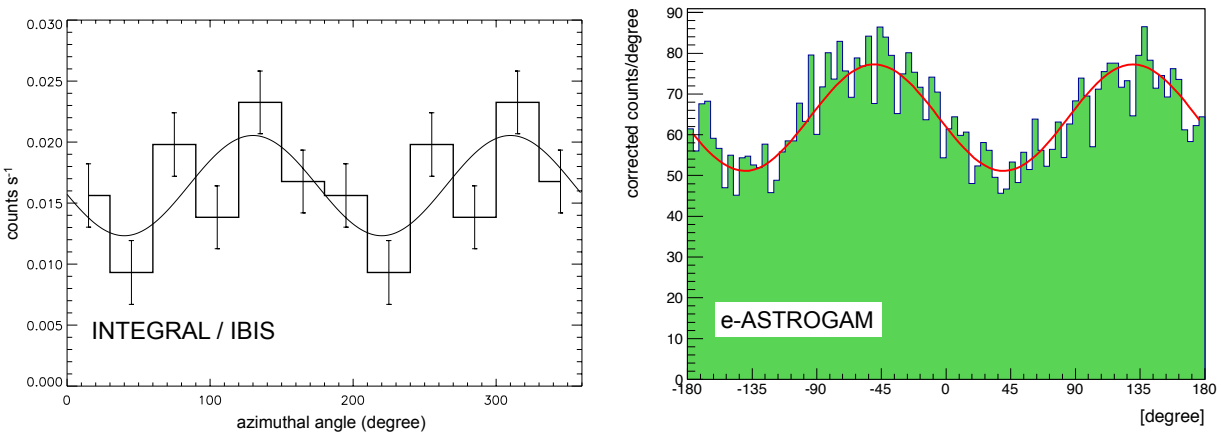

(a) (b)

Fig 8 Similar to Fig. 6, but for the black hole binary Cygnus X-1 in the low hard state (LHS). (a) Polarization diagram obtained with *INTEGRAL*/IBIS in the 400 – 2000 keV energy band by summing 2.05 Ms of data accumulated between May 2003 and May 2014 (adapted from Ref. 56). The measured polarization fraction and angle are $\mathrm{PF} = (75 \pm 32)\%$ and $\mathrm{PA} = 40.0^\circ \pm 14.3^\circ$, respectively. (b) Simulation of the e-ASTROGAM polarization signal in the same energy band (400 – 2000 keV) for an effective duration of observation of Cyg X-1 in the hard state 100 times shorter than that accumulated by *INTEGRAL*/IBIS (i.e. $T_{\mathrm{obs}} = 2.05 \times 10^4$ s). The reconstructed polarization fraction and angle are $\mathrm{PF} = (75.0 \pm 4.7)\%$ and $\mathrm{PA} = 41.2^\circ \pm 1.9^\circ$.

range. This has been recently confirmed by the two main instruments on board the *INTEGRAL* observatory, IBIS and SPI.[54,55] Both teams have demonstrated that the 400 – 2000 keV emission in Cyg X-1 is polarized at a level of about 70%, while only a 20% upper limit on the degree of polarization was obtained at lower energies. It has been suggested that the polarized emission is due to synchrotron emission from the compact jet. This result is important for our understanding of the accretion-ejection process.

Figure 8 shows a comparison of a polarization diagram for Cygnus X-1 in the LHS obtained with *INTEGRAL*/IBIS summing 2.05 Ms of data,[56] and a simulated polarigramme for e-ASTROGAM observation of Cyg X-1 in the LHS with 100 times shorter exposure ($T_{\mathrm{obs}} = 2.05 \times 10^4$ s). For the simulations the energy spectrum of Cyg X-1 in the LHS measured by Rodriguez et al.[56] was used, along with the central values obtained by these authors with *INTEGRAL*/IBIS for the polarization fraction ($\mathrm{PF} = 75.0\%$) and angle ($\mathrm{PA} = 40.0^\circ$) in the energy

range 400 – 2000 keV. The simulated result shows that e-ASTROGAM will be able to provide a detailed spectral and time-resolved gamma-ray view of the polarization properties of Cyg X-1, thus answering questions regarding the different emitting media in those sources (Comptonized corona vs. synchrotron-self Compton jets), while providing important clues concerning the composition, energetics and magnetic field of the jet.

The excellent sensitivity of e-ASTROGAM in the MeV range will also give access to detailed studies of other, fainter, microquasars (e.g. GRS 1915+105, 1E1740.7-2942, GRS 1758-258, GRO J1655-40), whose polarized gamma-ray emission is not currently detectable.

4 Conclusions

The e-ASTROGAM gamma-ray telescope is based on an innovative design allowing measurements of the energy and 3D position of each interaction within the detectors with excellent spectral and spatial resolution, while minimizing passive material in the detector volume. With these features, e-ASTROGAM will be able to perform unprecedented polarization measurements in the MeV range using Compton interactions in the instrument. In the pair domain, a precise evaluation of the instrument polarimetric performance will require more detailed simulations. But preliminary estimates suggest that a 5σ minimum detectable polarization of ≈ 20 – 40% in the energy range from 10 to 100 MeV should be within reach for bright gamma-ray sources such as the Vela and Crab pulsars (see Ref. 5).

e-ASTROGAM polarization sensitivity will complement the polarization studies at lower energies, such that of the IXPE mission, which is currently under construction at NASA.[57] That mission, however, will be sensitive in the 1 – 10 keV band, and together, the data from both missions will afford polarization measurements over an unprecedented spectral range.

The polarimetry capabilities of e-ASTROGAM will be crucial for a variety of investigations. Thus, it will bring a new diagnostic of gamma-ray emission models in all classes of AGN, with the potential to clearly identify the presence of hadrons in jets of BL Lac blazars, which are considered as a possible source of ultra-high-energy cosmic rays. In GRBs, polarization information can place strong new observational constraints on the nature of the ultrarelativistic outflow, its geometry and magnetization, as well as on the high-energy radiation mechanisms; measurements of GRB polarization also have the potential to provide constraining limits on violation of Lorentz invariance. e-ASTROGAM polarimetric studies of gamma-ray emission from compact objects will help to understand the new type of particle acceleration identified in the Crab nebula.[43,58] In microquasars, e-ASTROGAM's sensitivity to polarization will make it possible to probe in detail the transition between accretion disks and relativistic jets, and will provide new insight into the composition, energetics and magnetic fields of these jets. For all of these studies, simulations of the e-ASTROGAM response to polarized photons show that the proposed space mission will be able to exploit, for the first time, the information encoded in the polarization of many types of cosmic gamma-ray sources.

Acknowledgments

The research leading to these results has received funding from the European Union's Horizon 2020 Programme under the AHEAD project (grant agreement n. 654215).

References

1 P. Laurent, D. Götz, P. Binétruy, *et al.*, "Constraints on Lorentz Invariance Violation using integral/IBIS observations of GRB041219A," *Physical Review D* **83**, 121301 (2011).

2 M. Tavani, G. Barbiellini, A. Argan, *et al.*, "The AGILE Mission," *Astronomy and Astrophysics* **502**, 995–1013 (2009).

3 W. B. Atwood, A. A. Abdo, M. Ackermann, *et al.*, "The Large Area Telescope on the Fermi Gamma-Ray Space Telescope Mission," *Astrophysical Journal* **697**, 1071–1102 (2009).

4 G. Kanbach, R. Andritschke, A. Zoglauer, *et al.*, "Development and calibration of the tracking Compton/Pair telescope MEGA," *Nuclear Instruments and Methods in Physics Research A* **541**, 310–322 (2005).

5 A. De Angelis, V. Tatischeff, M. Tavani, *et al.*, "The e-ASTROGAM mission (exploring the extreme Universe with gamma rays in the MeV-GeV range)," *ArXiv e-prints* (2016).

6 R. Campana, M. Orlandini, E. Del Monte, *et al.*, "The radiation environment in a low earth orbit:the case of BeppoSAX," *Experimental Astronomy* **37**, 599–613 (2014).

7 A. Zoglauer, R. Andritschke, and F. Schopper, "MEGAlib The Medium Energy Gamma-ray Astronomy Library," *New Astronomy Reviews* **50**, 629–632 (2006).

8 A. Bulgarelli, V. Fioretti, P. Malaguti, *et al.*, "BoGEMMS: the Bologna Geant4 multi-mission simulator," in *High Energy, Optical, and Infrared Detectors for Astronomy V*, *Proceedings of the SPIE* **8453**, 845335 (2012).

9 V. Tatischeff, M. Tavani, P. von Ballmoos, *et al.*, "The e-ASTROGAM gamma-ray space mission," in *Society of Photo-Optical Instrumentation Engineers (SPIE) Conference Series*, *Proceedings of the SPIE* **9905**, 99052N (2016).

10 D. Bernard, "Polarimetry of cosmic gamma-ray sources above e^+e^- pair creation threshold," *Nuclear Instruments and Methods in Physics Research A* **729**, 765–780 (2013).

11 G. . Madejski and M. Sikora, "Gamma-Ray Observations of Active Galactic Nuclei," *Annual Review of Astronomy and Astrophysics* **54**, 725–760 (2016).

12 M. Ackermann, M. Ajello, A. Allafort, *et al.*, "Search for Gamma-ray Emission from X-Ray-selected Seyfert Galaxies with Fermi-LAT," *Astrophysical Journal* **747**, 104 (2012).

13 M. Ackermann, M. Ajello, A. Allafort, *et al.*, "GeV Observations of Star-forming Galaxies with the Fermi Large Area Telescope," *Astrophysical Journal* **755**, 164 (2012).

14 W. N. Johnson, A. A. Zdziarski, G. M. Madejski, *et al.*, "Seyferts and radio galaxies," in *Proceedings of the Fourth Compton Symposium*, C. D. Dermer, M. S. Strickman, and J. D. Kurfess, Eds., *American Institute of Physics Conference Series* **410**, 283–305 (1997).

15 P. Lubiński, V. Beckmann, L. Gibaud, *et al.*, "A comprehensive analysis of the hard X-ray spectra of bright Seyfert galaxies," *Monthly Notices of the Royal Astronomical Society* **458**, 2454–2475 (2016).

16 G. Tagliaferri, G. Ghisellini, M. Perri, *et al.*, "NuSTAR and Multifrequency Study of the Two High-redshift Blazars S5 0836+710 and PKS 2149-306," *Astrophysical Journal* **807**, 167 (2015).

17 M. Ackermann, R. Anantua, K. Asano, *et al.*, "Minute-timescale > 100 MeV γ-Ray Variability during the Giant Outburst of Quasar 3C 279 Observed by Fermi-LAT in 2015 June," *Astrophysical Journal* **824**, L20 (2016).

18 M. Sikora, M. C. Begelman, and M. J. Rees, "Comptonization of diffuse ambient radiation by a relativistic jet: The source of gamma rays from blazars?," *Astrophysical Journal* **421**, 153–162 (1994).

19 M. Sikora, Ł. Stawarz, R. Moderski, *et al.*, "Constraining Emission Models of Luminous Blazar Sources," *Astrophysical Journal* **704**, 38–50 (2009).

20 H. Krawczynski, "The Polarization Properties of Inverse Compton Emission and Implications for Blazar Observations with the GEMS X-Ray Polarimeter," *Astrophysical Journal* **744**, 30 (2012).

21 K. Nalewajko, M. C. Begelman, B. Cerutti, *et al.*, "Energetic constraints on a rapid gamma-ray flare in PKS 1222+216," *Monthly Notices of the Royal Astronomical Society* **425**, 2519–2529 (2012).

22 N. Chakraborty, V. Pavlidou, and B. D. Fields, "High Energy Polarization of Blazars: Detection Prospects," *Astrophysical Journal* **798**, 16 (2015).

23 H. Zhang and M. Böttcher, "X-Ray and Gamma-Ray Polarization in Leptonic and Hadronic Jet Models of Blazars," *Astrophysical Journal* **774**, 18 (2013).

24 H. Zhang, C. Diltz, and M. Böttcher, "Radiation and Polarization Signatures of the 3D Multizone Time-dependent Hadronic Blazar Model," *Astrophysical Journal* **829**, 69 (2016).

25 N. Gehrels and S. Razzaque, "Gamma-ray bursts in the swift-Fermi era," *Frontiers of Physics* **8**, 661–678 (2013).

26 E. Berger, "Short-Duration Gamma-Ray Bursts," *Annual Review of Astronomy and Astrophysics* **52**, 43–105 (2014).

27 K. Toma, T. Sakamoto, B. Zhang, *et al.*, "Statistical Properties of Gamma-Ray Burst Polarization," *Astrophysical Journal* **698**, 1042–1053 (2009).

28 C. Lundman, A. Pe'er, and F. Ryde, "Polarization properties of photospheric emission from

relativistic, collimated outflows," *Monthly Notices of the Royal Astronomical Society* **440**, 3292–3308 (2014).

29 S. McGlynn, D. J. Clark, A. J. Dean, *et al.*, "Polarisation studies of the prompt gamma-ray emission from GRB 041219a using the spectrometer aboard INTEGRAL," *Astronomy & Astrophysics* **466**, 895–904 (2007).

30 D. Götz, P. Laurent, F. Lebrun, *et al.*, "Variable Polarization Measured in the Prompt Emission of GRB 041219A Using IBIS on Board INTEGRAL," *Astrophysical Journal* **695**, L208–L212 (2009).

31 D. Yonetoku, T. Murakami, S. Gunji, *et al.*, "Gamma-Ray Burst Polarimeter (GAP) aboard the Small Solar Power Sail Demonstrator IKAROS," *Publications of the Astronomical Society of Japan* **63**, 625–638 (2011).

32 D. Yonetoku, T. Murakami, S. Gunji, *et al.*, "Detection of Gamma-Ray Polarization in Prompt Emission of GRB 100826A," *Astrophysical Journal* **743**, L30 (2011).

33 D. Yonetoku, T. Murakami, S. Gunji, *et al.*, "Magnetic Structures in Gamma-Ray Burst Jets Probed by Gamma-Ray Polarization," *Astrophysical Journal* **758**, L1 (2012).

34 M. L. McConnell, M. Baring, P. Bloser, *et al.*, "POET: a SMEX mission for gamma ray burst polarimetry," in *Space Telescopes and Instrumentation 2014: Ultraviolet to Gamma Ray*, *Proceedings of the SPIE* **9144**, 91440O (2014).

35 T. P. Connor, C. M. Bancroft, P. F. Bloser, *et al.*, "Plans for the first balloon flight of the gamma-ray polarimeter experiment (GRAPE)," in *Space Telescopes and Instrumentation 2010: Ultraviolet to Gamma Ray*, *Proceedings of the SPIE* **7732**, 77324E (2010).

36 S. Xiong, N. Produit, and B. Wu, "Expected performance of a hard X-ray polarimeter (POLAR) by Monte Carlo simulation," *Nuclear Instruments and Methods in Physics Research A* **606**, 552–559 (2009).

37 S. V. Vadawale, T. Chattopadhyay, A. R. Rao, *et al.*, "Hard X-ray polarimetry with Astrosat-CZTI," *Astronomy and Astrophysics* **578**, A73 (2015).

38 A. R. Rao, V. Chand, M. K. Hingar, *et al.*, "AstroSat CZT Imager Observations of GRB 151006A: Timing, Spectroscopy, and Polarization Study," *Astrophysical Journal* **833**, 86 (2016).

39 D. Band, J. Matteson, L. Ford, *et al.*, "BATSE observations of gamma-ray burst spectra. I - Spectral diversity," *Astrophysical Journal* **413**, 281–292 (1993).

40 M. C. Weisskopf, R. F. Elsner, D. Hanna, *et al.*, "The prospects for X-ray polarimetry and its potential use for understanding neutron stars," *ArXiv Astrophysics e-prints* (2006).

41 W. S. Paciesas, C. A. Meegan, G. N. Pendleton, *et al.*, "The Fourth BATSE Gamma-Ray Burst Catalog (Revised)," *Astrophysical Journal Supplement* **122**, 465–495 (1999).

42 A. A. Abdo, M. Ackermann, M. Ajello, *et al.*, "Gamma-Ray Flares from the Crab Nebula," *Science* **331**, 739 (2011).

43 M. Tavani, A. Bulgarelli, V. Vittorini, *et al.*, "Discovery of Powerful Gamma-Ray Flares from the Crab Nebula," *Science* **331**, 736 (2011).

44 E. Striani, M. Tavani, V. Vittorini, *et al.*, "Variable Gamma-Ray Emission from the Crab Nebula: Short Flares and Long "Waves"," *Astrophysical Journal* **765**, 52 (2013).

45 M. C. Weisskopf, E. H. Silver, H. L. Kestenbaum, *et al.*, "A precision measurement of the

X-ray polarization of the Crab Nebula without pulsar contamination," *Astrophysical Journal* **220**, L117–L121 (1978).

46 M. Forot, P. Laurent, I. A. Grenier, *et al.*, "Polarization of the Crab Pulsar and Nebula as Observed by the INTEGRAL/IBIS Telescope," *Astrophysical Journal* **688**, L29 (2008).

47 A. J. Dean, D. J. Clark, J. B. Stephen, *et al.*, "Polarized Gamma-Ray Emission from the Crab," *Science* **321**, 1183 (2008).

48 P. Moran, G. Kyne, C. Gouiffès, *et al.*, "A recent change in the optical and γ-ray polarization of the Crab nebula and pulsar," *Monthly Notices of the Royal Astronomical Society* **456**, 2974–2981 (2016).

49 E. Jourdain and J. P. Roques, "The High-Energy Emission of the Crab Nebula from 20 keV TO 6 MeV with Integral SPI," *Astrophysical Journal* **704**, 17–24 (2009).

50 A. A. Abdo, M. Ackermann, M. Ajello, *et al.*, "A change in the optical polarization associated with a γ-ray flare in the blazar 3C279," *Nature* **463**, 919–923 (2010).

51 S. Bowyer, E. T. Byram, T. A. Chubb, *et al.*, "Cosmic X-ray sources," *Science* **147**, 394 (1965).

52 C. T. Bolton, "Orbital elements and an analysis of models for HDE 226868 = Cygnus X-1," *Astrophysical Journal* **200**, 269 (1975).

53 A. M. Stirling, R. E. Spencer, C. J. de la Force, *et al.*, "A relativistic jet from Cygnus X-1 in the low/hard X-ray state," *Monthly Notices of the Royal Astronomical Society* **327**, 1273 (2001).

54 P. Laurent, J. Rodriguez, J. Wilms, *et al.*, "Polarized Gamma-Ray Emission from the Galactic Black Hole Cygnus X-1," *Science* **332**, 438 (2011).

55 E. Jourdain, J. P. Roques, M. Chauvin, *et al.*, "Separation of Two Contributions to the High Energy Emission of Cygnus X-1: Polarization Measurements with INTEGRAL SPI," *Astrophysical Journal* **761**, 27 (2012).

56 J. Rodriguez, V. Grinberg, P. Laurent, *et al.*, "Spectral State Dependence of the 0.4-2 MeV Polarized Emission in Cygnus X-1 Seen with INTEGRAL/IBIS, and Links with the AMI Radio Data," *Astrophysical Journal* **807**, 17 (2015).

57 M. C. Weisskopf, B. Ramsey, S. O'Dell, *et al.*, "The Imaging X-ray Polarimetry Explorer (IXPE)," in *Space Telescopes and Instrumentation 2016: Ultraviolet to Gamma Ray*, *Proceedings of the SPIE* **9905**, 990517 (2016).

58 M. Tavani, "Super-Acceleration in the Flaring Crab Nebula," *Nuclear Physics B Proceedings Supplements* **243**, 131–140 (2013).